Variations of atmospheric muons and background measured with Large Volume Detector

Natalia Agafonova (INR RAS),
N.A. Filimonova, E.A. Dobrynina, O.G. Ryazhskaya, I.R. Shakyrianova, V.V. Ashikhmin, V.F. Yakushev, R.I. Enikeev
and **LVD Collaboration**

ISCRA 2021, June 08-10, 2021

LVD – Large Volume Detector at LNGS, Italy, Gran Sasso

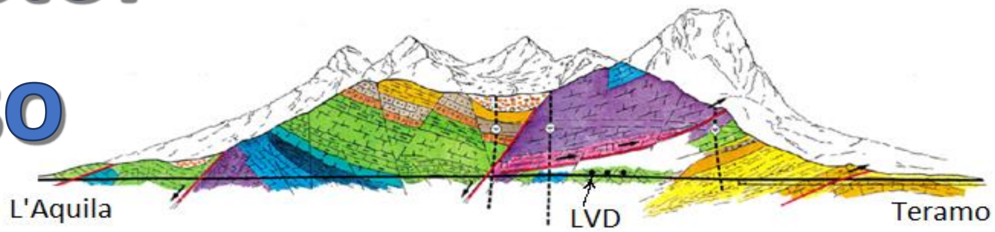

The main goal of LVD is searching for neutrino radiation from stellar core collapse.

The coordinates of the LNGS: 13.5333 E, 42.4275 N.

Length ×Width ×Height	22.7×13.2×10 m
Iron mass	1020 t
Scintillator mass	1008 t
Amount of scintillation counters	840
Average depth minimal	3620 m w.e. 3000 m w.e.
Mean muon energy	280 GeV
E_μ on see level (min.)	1.3 TeV
Muon rate (on 1 tower)	~ 120 h^{-1}
Threshold ε_{th}	4 MeV

Atmospheric muons detection

The average Muon counting rate

$R_{\mu}(LVD) = 0.097 \pm 0.010\ s^{-1}$

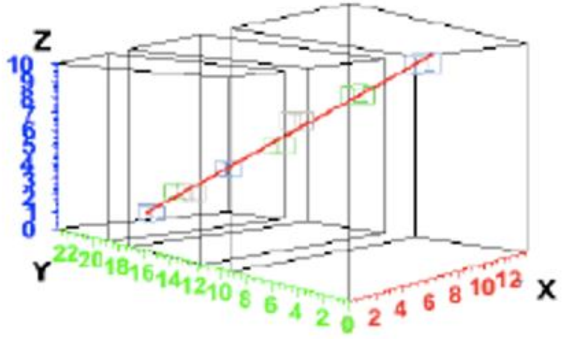

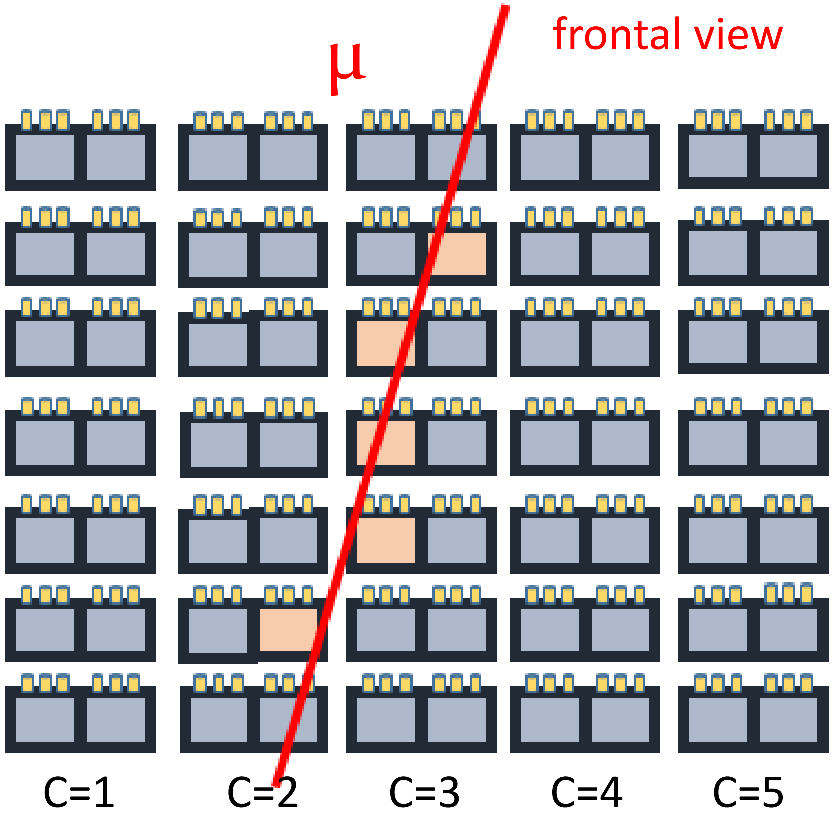

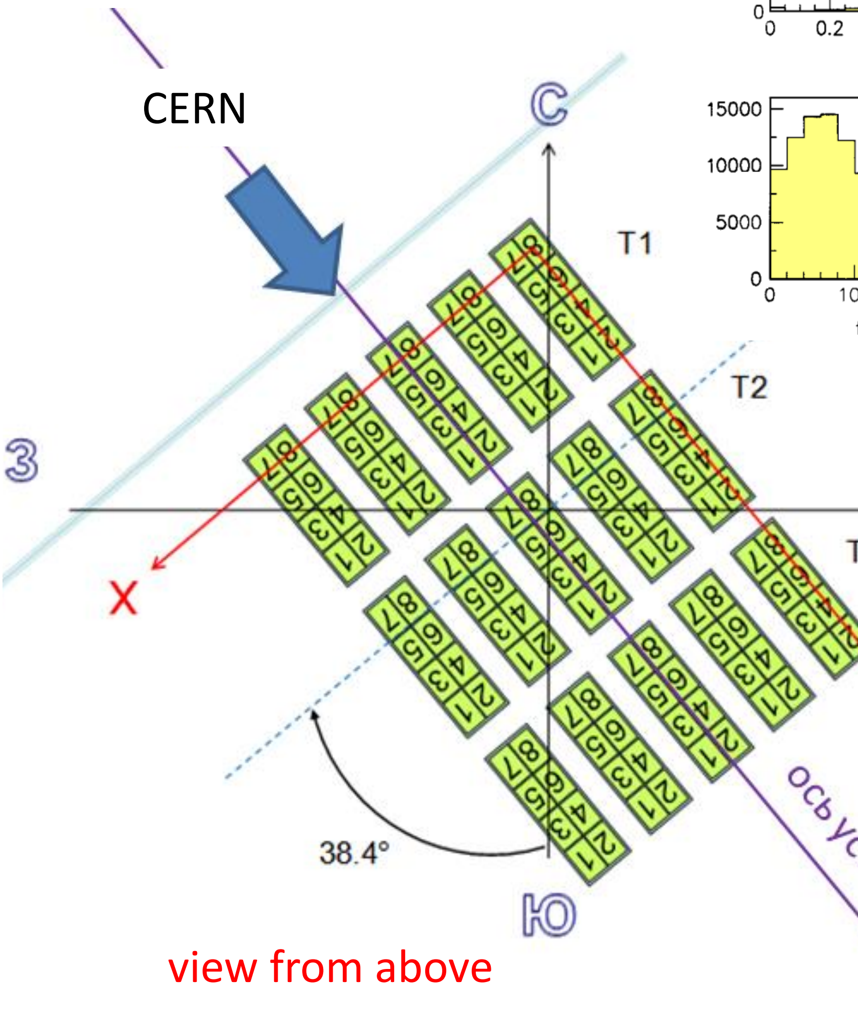

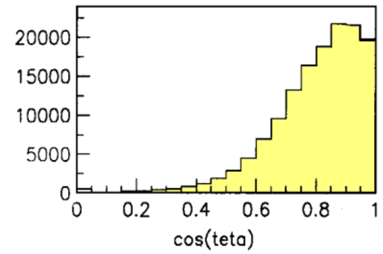

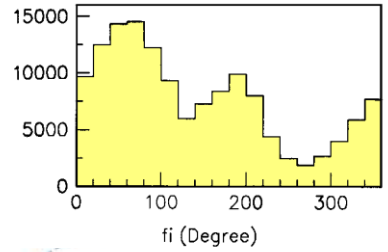

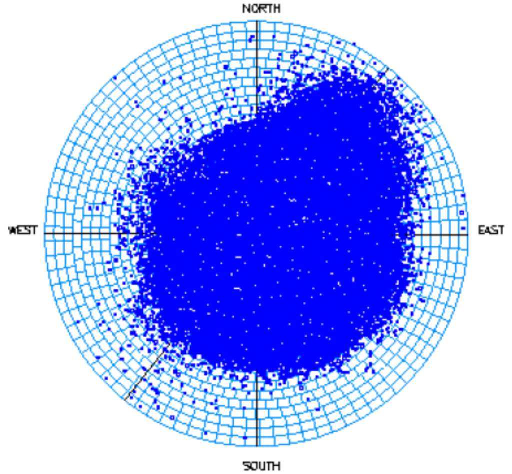

Maximum intensity angle $\theta=28°$

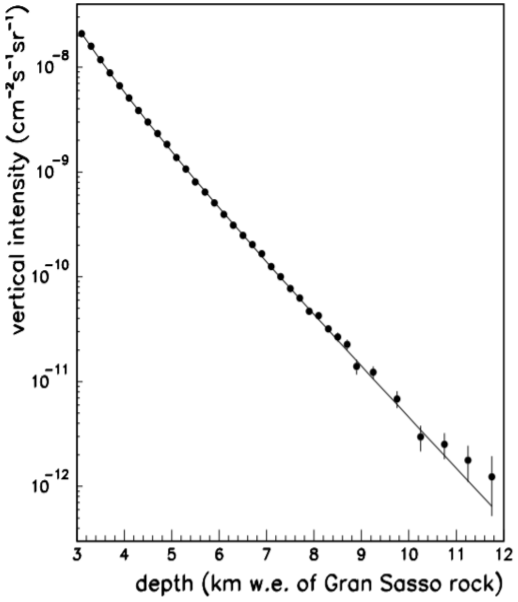

Variations of atmospheric muons

*N. Agafonova et al. (LVD Collaboration) "**Characterization of the varying flux of atmospheric muons measured with the Large Volume Detector for 24 years**", Phys. Rev. D 100, 062002 (2019)*

$\alpha_T = 0.93 \pm 0.02$

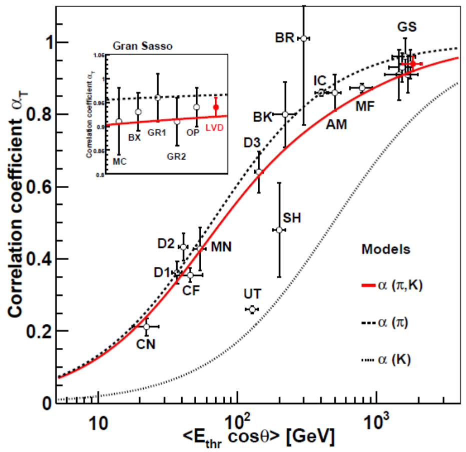

$$\Delta I_\mu / I_\mu^0 = \alpha_T \frac{\Delta T_{eff}}{T^0_{eff}}$$

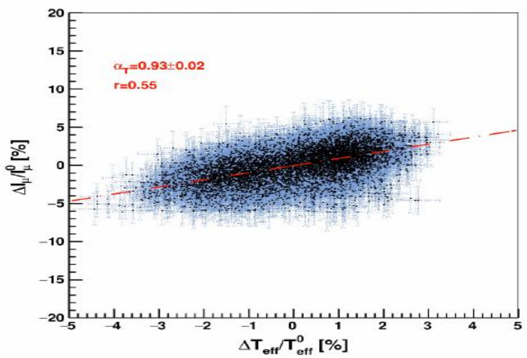

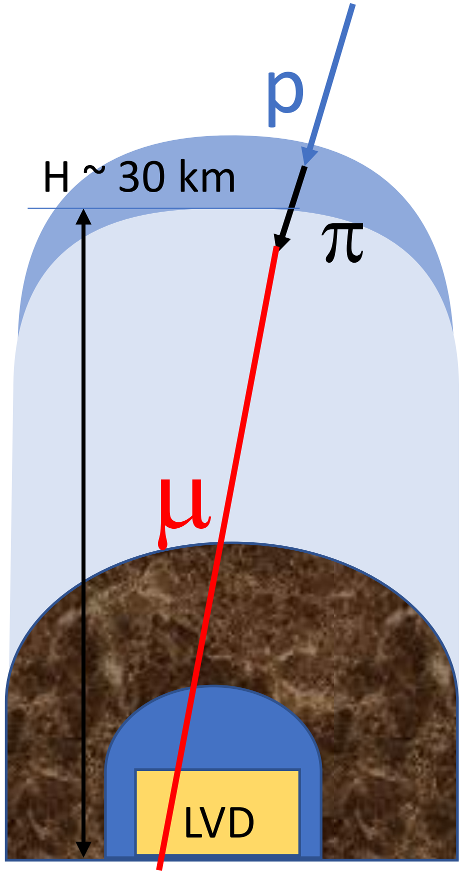

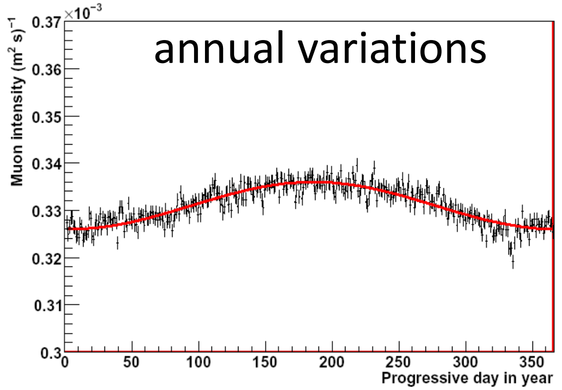

$$I_\mu = I_0^\mu + \delta I^\mu \cos\left(\frac{2\pi}{T}(t - t_0)\right)$$

Muons that reach great depths are produced, generally, in the **decays of pions of the first generation**.

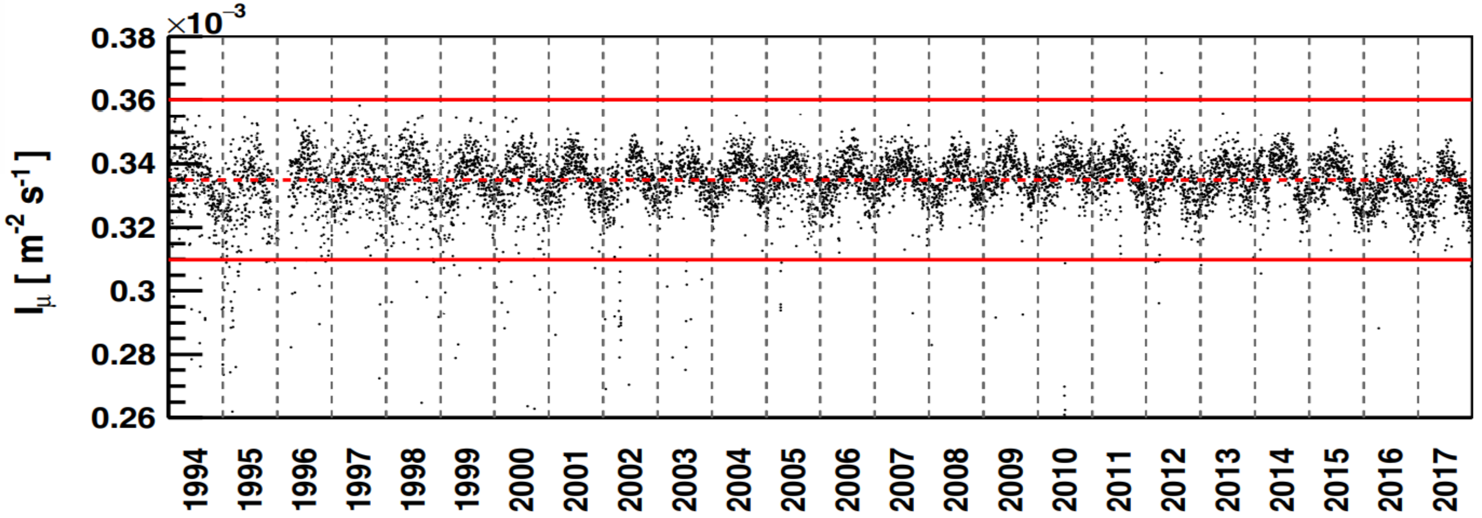

Average muon flux

$$I_\mu = (3.35 \pm 0.0005^{stat} \pm 0.03^{sys}) \times 10^{-4}\ m^{-2}\ s^{-1}$$

Low-energy Background

A dominant source of the background at underground laboratories in the range of low energies (0.5–5 MeV) are the spontaneous fission of uranium and thorium nuclei entering into the composition of the rock and setup materials, as well as their daughter nuclei. They create a flux of background photons and, to a smaller extent, neutrons.

Monitoring of radon concentrations is possible owing to the detection of gammas from decays of daughter nuclei of the radon isotope ^{222}Rn.

$$^{222}_{86}\mathrm{Rn} \xrightarrow{\alpha} {}^{218}_{84}\mathrm{Po} \xrightarrow{\alpha} {}^{214}_{82}\mathrm{Pb} \xrightarrow{\beta} {}^{214}_{83}\mathrm{Bi} \xrightarrow{\beta} {}^{214}_{84}\mathrm{Po} \xrightarrow{\alpha} {}^{210}_{82}\mathrm{Pb}$$

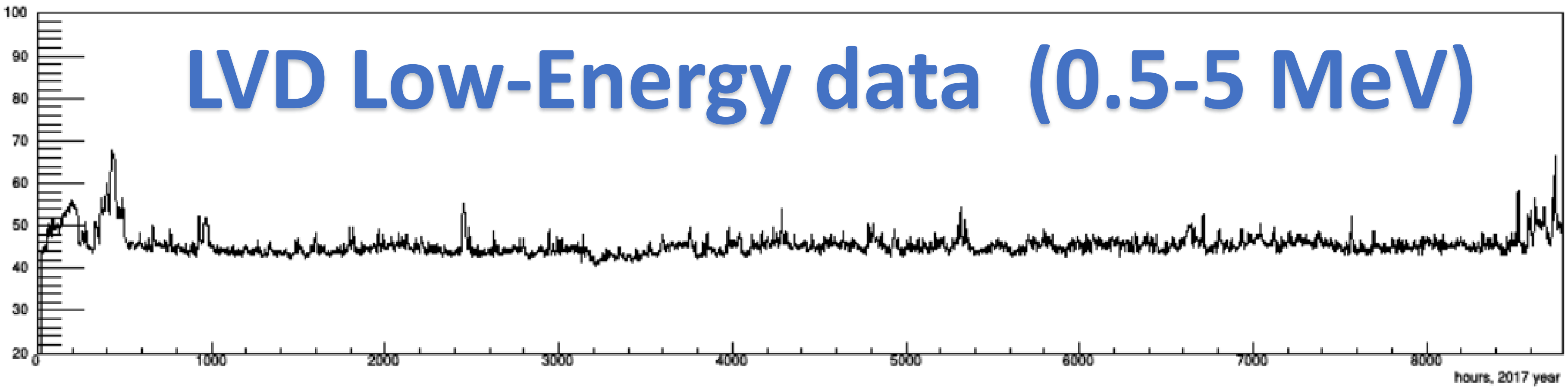

Gamma radiation is created, mainly, by bismuth (Bi) nuclei, due to β-decay transforming into polonium (Po) with a characteristic time of 19.7 min. **The energy spectrum of the gammas-radiation covers the range from 0.6 to 2.44 MeV**.

High-energy Background

Single trigger (E> 5 MeV) pulses in detector
- no muons,
- no muon bundles

Neutron from αn-reaction, Isolated cg-neutron from muons

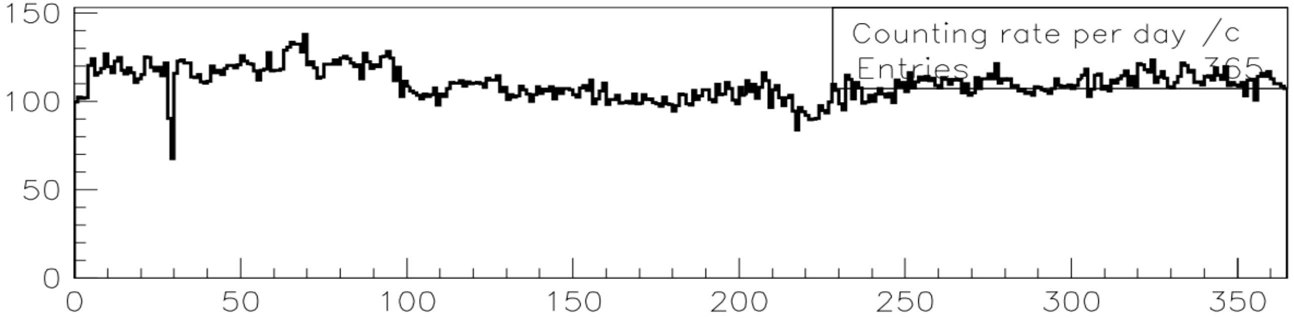

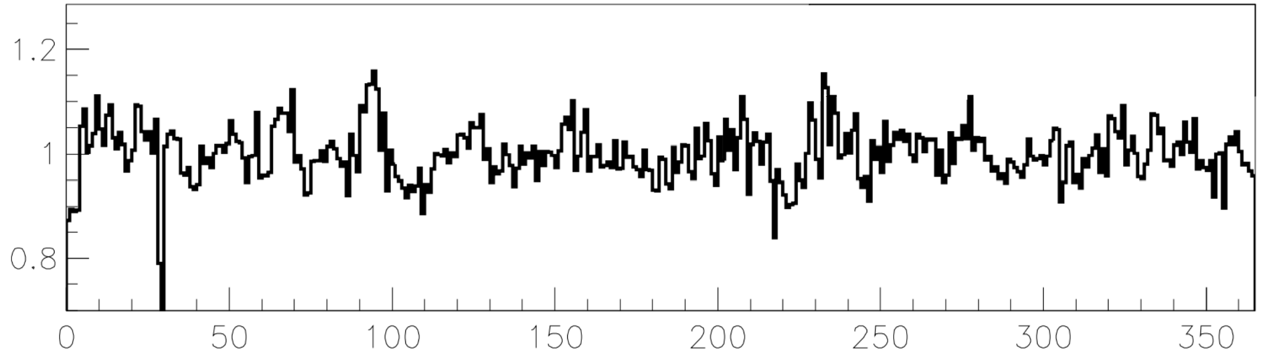

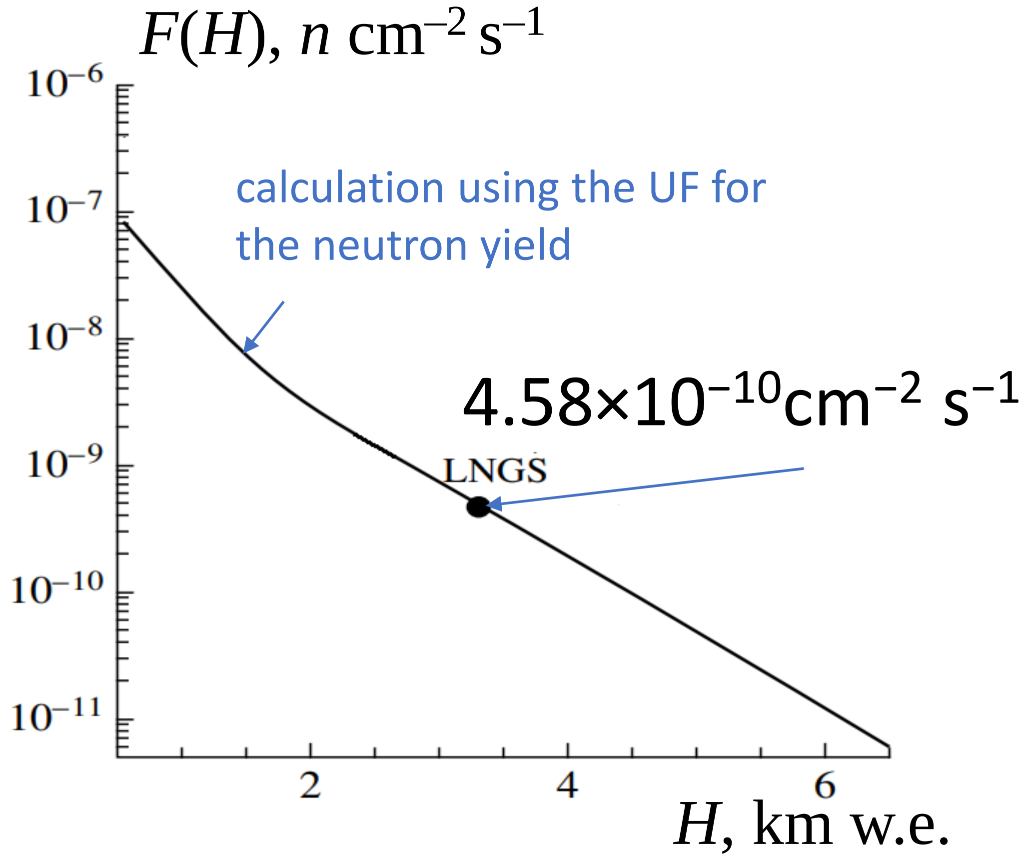

Total flux of muon induced neutrons in rock

$$F(H) = I_{\mu}(H)Y_{n}(H)l_{n}\rho\ [n\ \mathrm{cm}^{-2}\ \mathrm{s}^{-1}].$$

$$Y_n = 4.4\cdot10^{-7}\ \bar{E}_{\mu}^{0.78}A^{0.95}\ n/\mu/\ (\mathrm{g/cm}^2)\ \text{- UF}$$

A.S. Malgin, Physics of Atomic Nuclei, 2015, Vol. 78, No. 7, pp. 835-839

Weekly and Daily low-energy background variations

Seasonal low-energy background variations

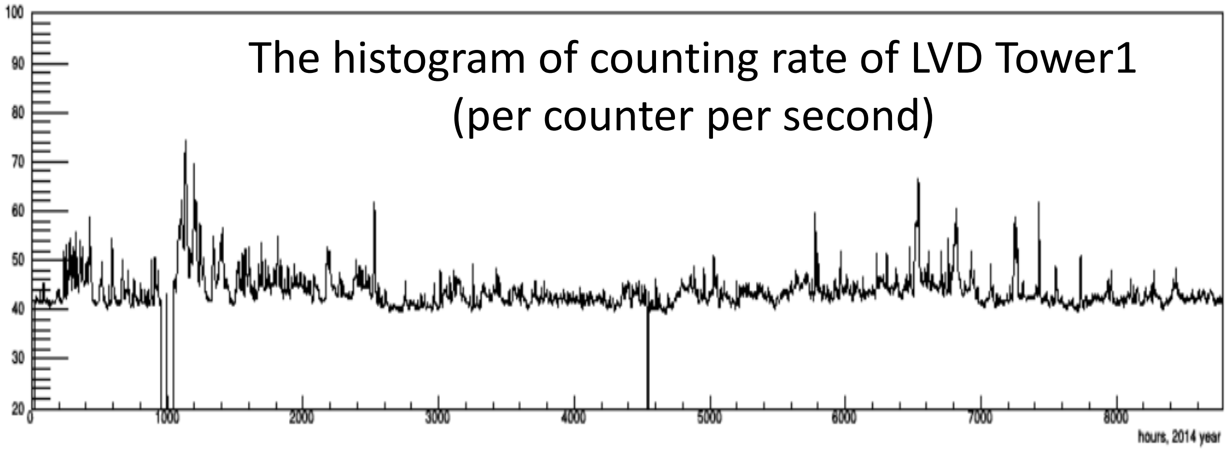

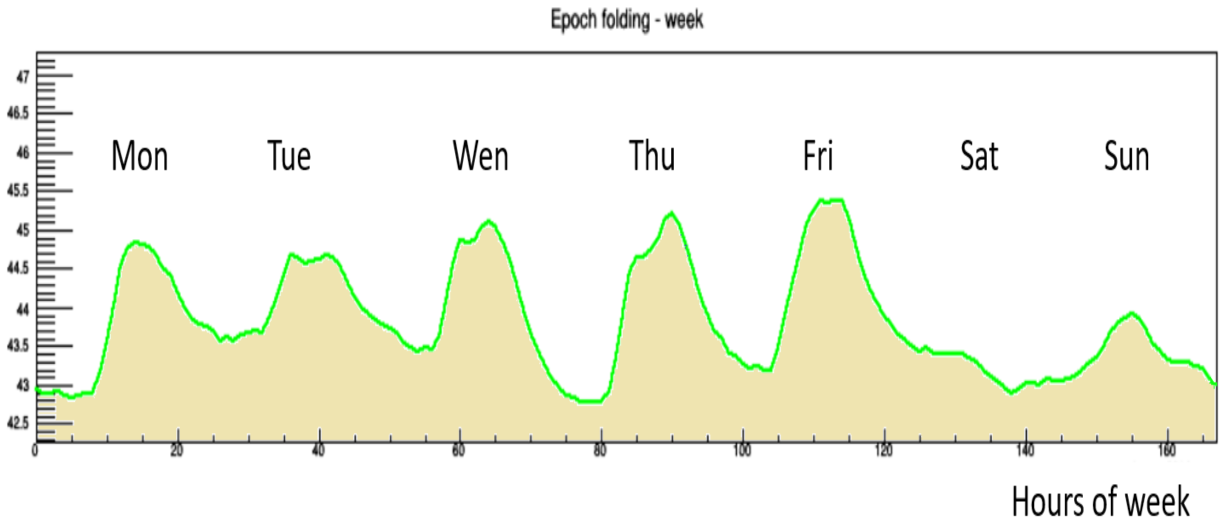

The modulation value is 4±2% and the phase is 8.1±0.4 months.

The maximum is **in early September**. Because radon is transported by underground waters, its maximum concentration is reached during the maximum saturation of the rock with water.

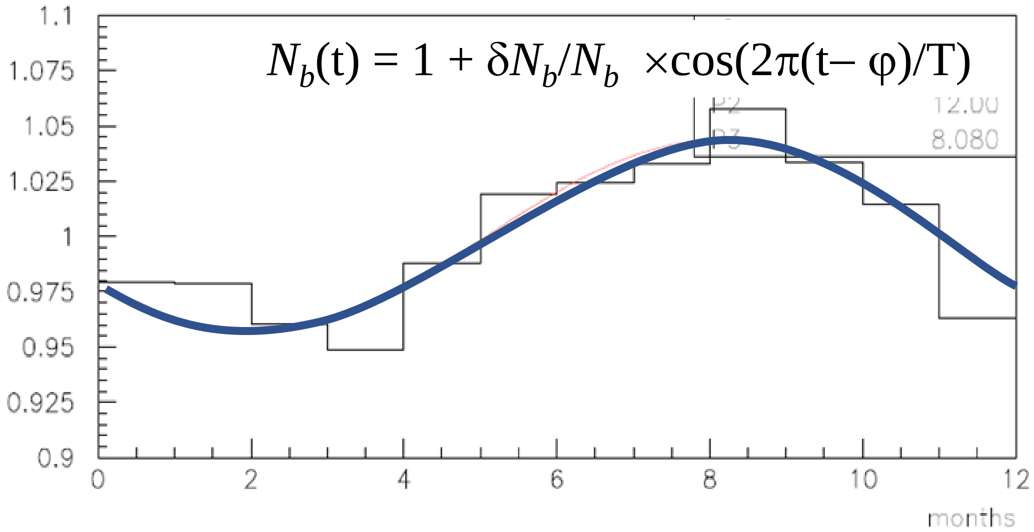

N.Yu Agafonova et al. Bulletin of the Russian Academy of Sciences: Physics, 2019, Vol. 83, No. 5, pp. 614–616

Atmospheric muons variation

$<E_\mu> \approx$ 270 GeV
$<H> \approx$ 3.3 km w.e.
$<\theta>$ $\approx$ 13°

$<E_\mu> \approx$ 340 GeV
$<H> \approx$ 5 km w.e.
$<\theta>$ $\approx$ 75°

δI_μ = (1.0±0.2) %
φ = 187 day = July, 6

δI_μ = (1.7± 0.3)%
φ = 182 day = July, 1

Neutrons from muons

$<E_n> \approx$ 1-12 MeV
From total muon direction°

δI_n = (7.7±0.8) %
φ = 6.9 month = July

Radon variation

E ~ 0.5–5 MeV,
sedimentary soil,
a lot of water

δI_b = (4±2) %
φ=8 month= September

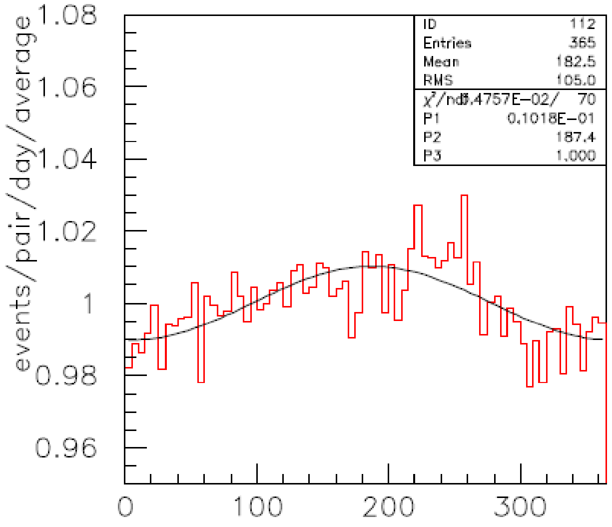

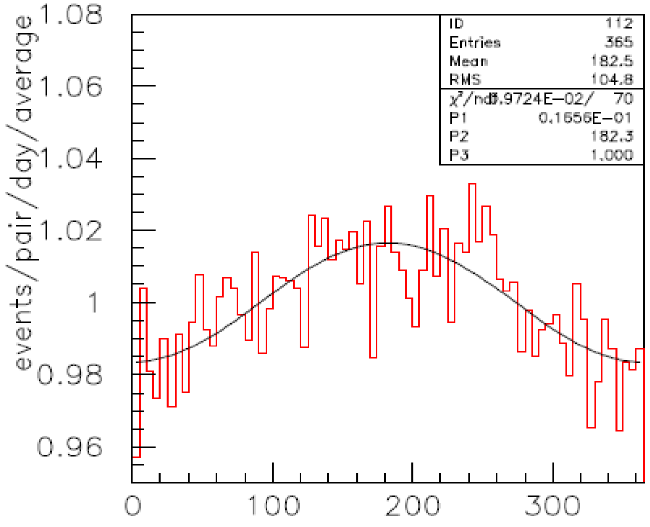

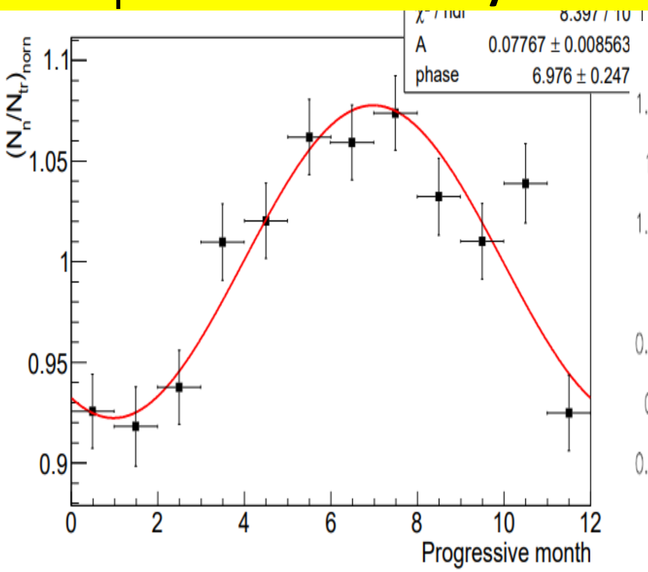

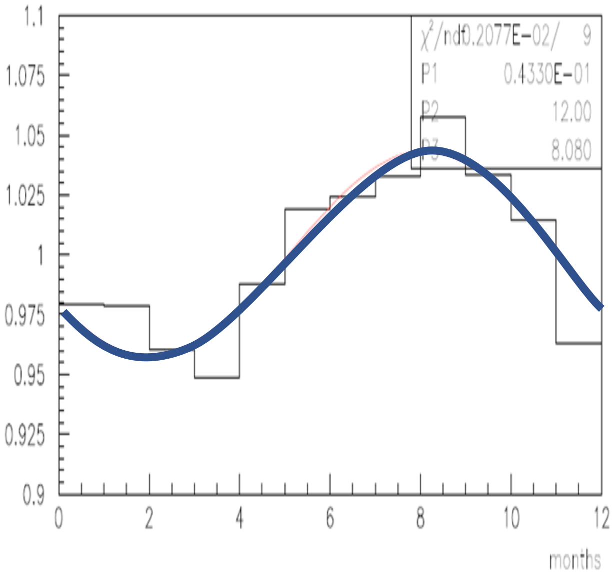

Agafonova N.Y., et al. Physics of Atomic Nuclei. 2020. T. 83. № 1. C. 69-74

Dependence on local atmospheric effects

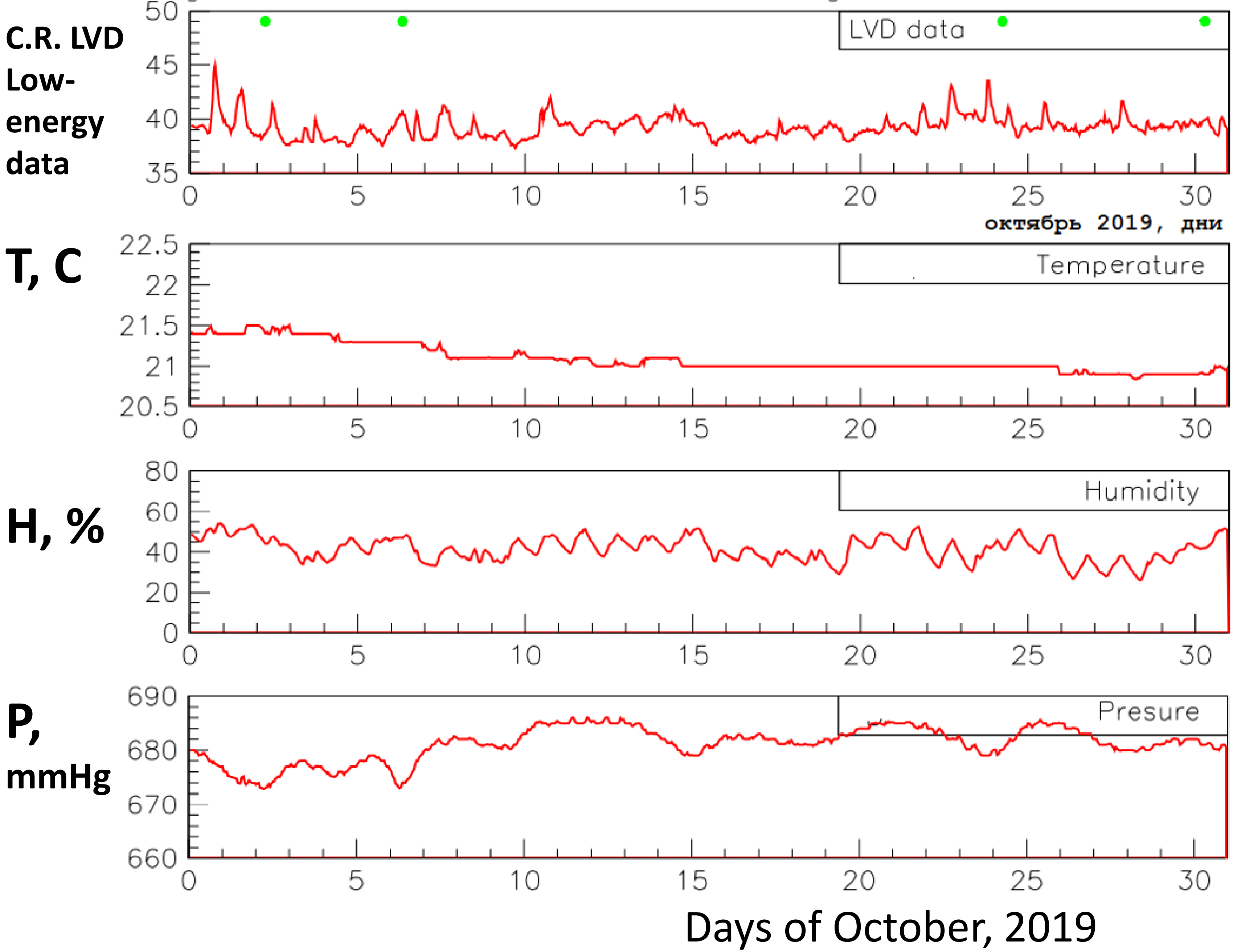

Low-energy background = “Radon background”

Comparative analysis of the counting rate of LVD (N_{LVD}) data at the lower threshold with local changes in temperature (T), humidity (H) and pressure (P). Peaks in Low Energy LVD (N_{LVD}) data are not associated with peaks in T, H, P.

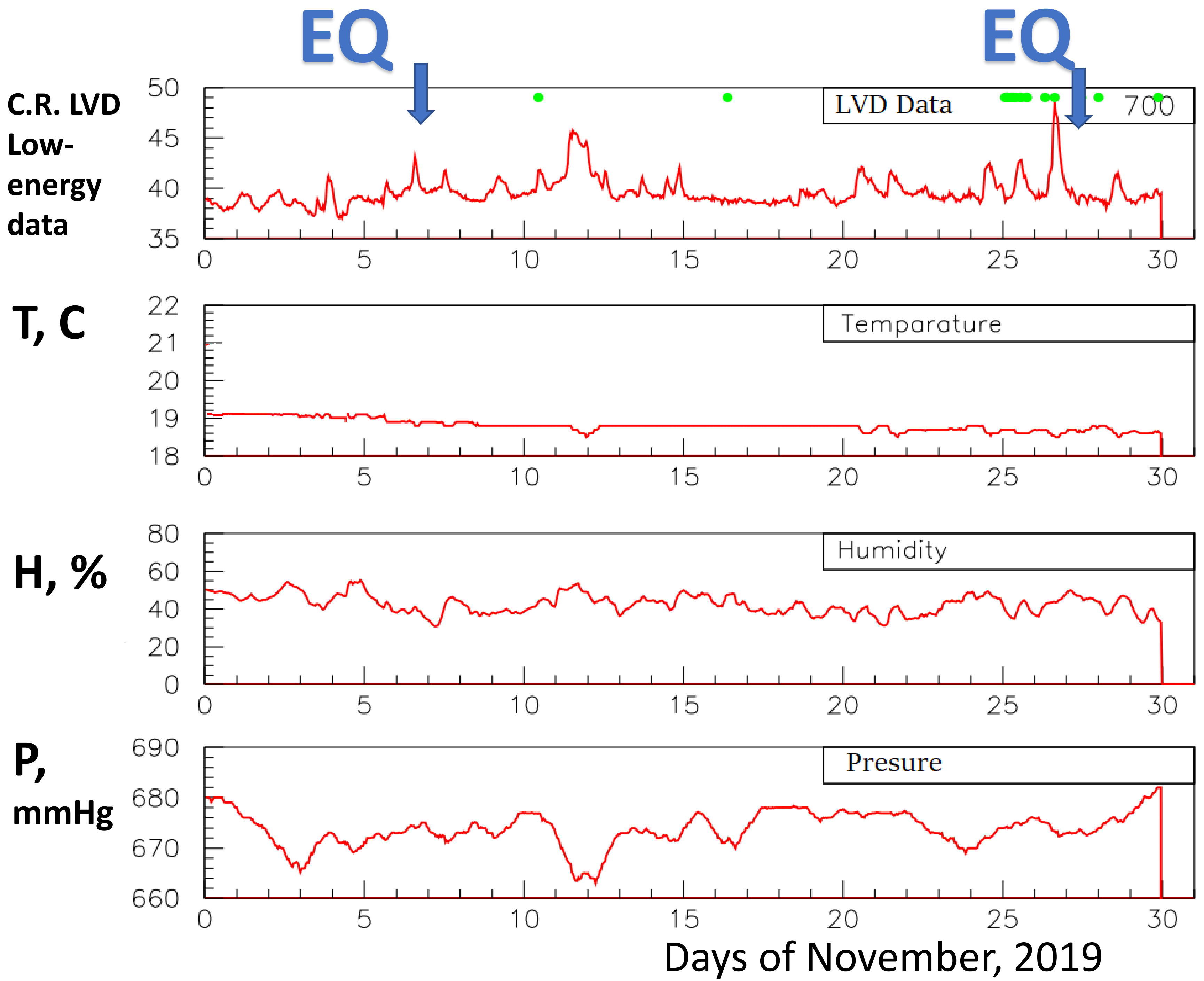
EQ
EQ
C.R. LVD Low-energy data
LVD Data
700
T, C
Temparature
H, %
Humidity
P, mmHg
Presure
50 45 40 35
22 21 20 19 18
80 60 40 20 0
690 680 670 660
0 5 10 15 20 25 30
Days of November, 2019

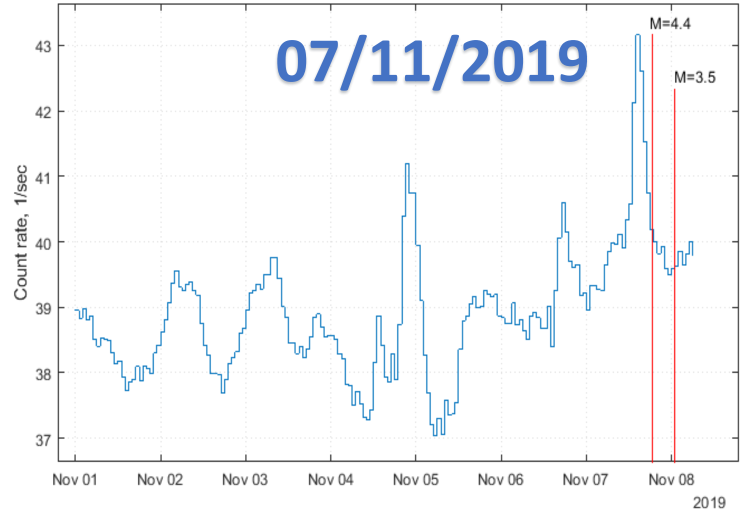
07/11/2019
M=4.4
M=3.5
Count rate, 1/sec
43 42 41 40 39 38 37
Nov 01 Nov 02 Nov 03 Nov 04 Nov 05 Nov 06 Nov 07 Nov 08
2019

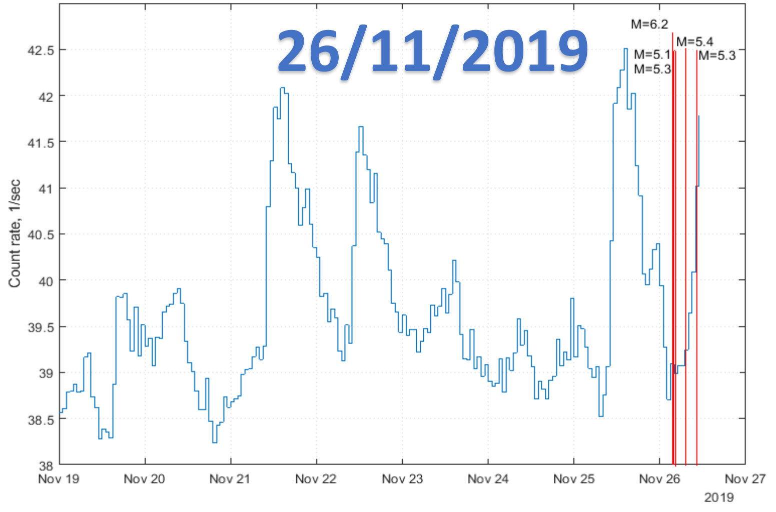
26/11/2019
M=6.2
M=5.4
M=5.1
M=5.3
M=5.3
Count rate, 1/sec
42.5 42 41.5 41 40.5 40 39.5 39 38.5 38
Nov 19 Nov 20 Nov 21 Nov 22 Nov 23 Nov 24 Nov 25 Nov 26 Nov 27
2019

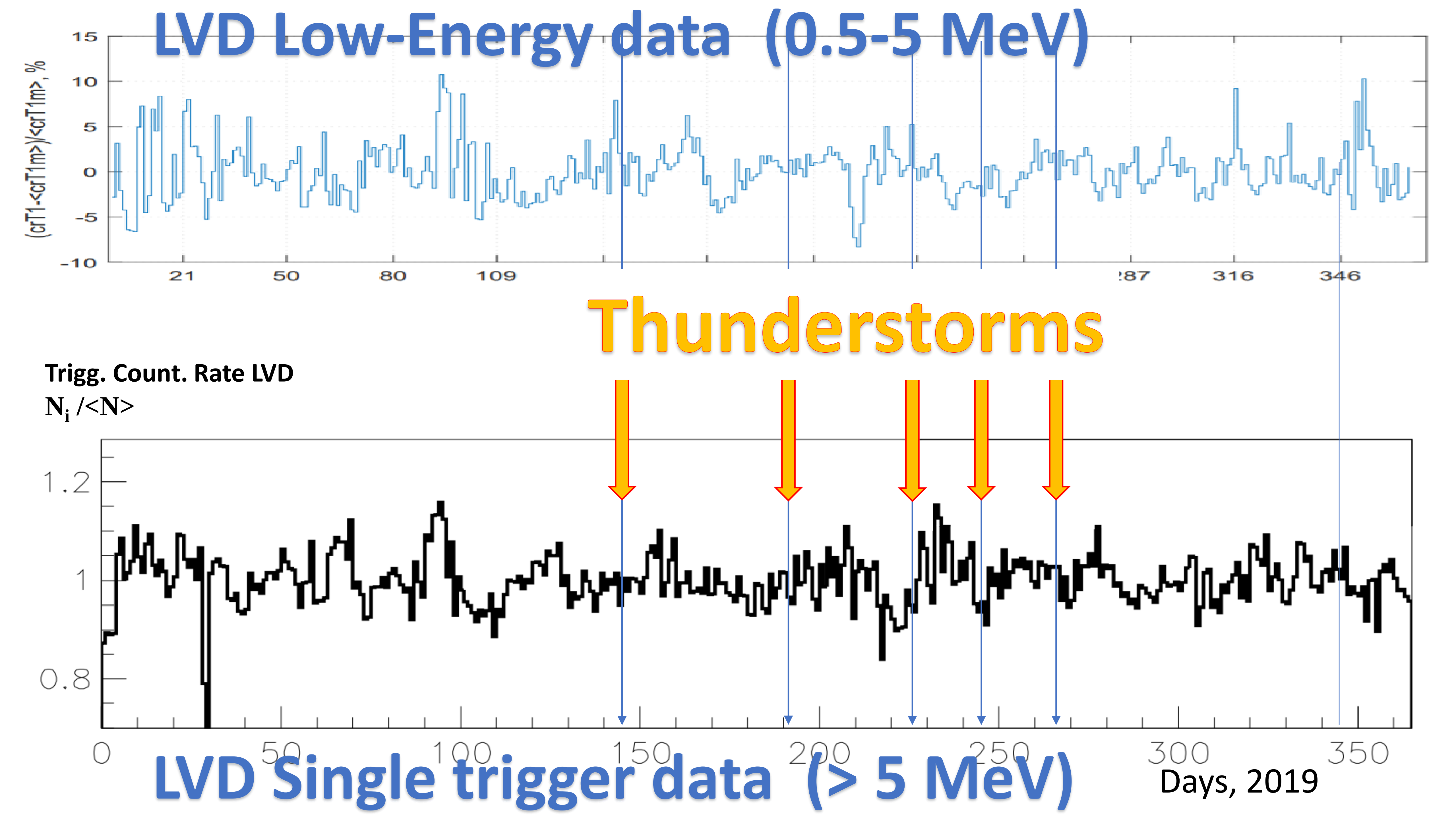
LVD Low-Energy data (0.5-5 MeV)
(crT1-<crT1m>)/<crT1m>, %
15
10
5
0
-5
-10
21
50
80
109
287
316
346
Thunderstorms
Trigg. Count. Rate LVD
N_i /<N>
1.2
1
0.8
0
50
100
150
200
250
300
350
Days, 2019
LVD Single trigger data (> 5 MeV)

Moon phases in 2019

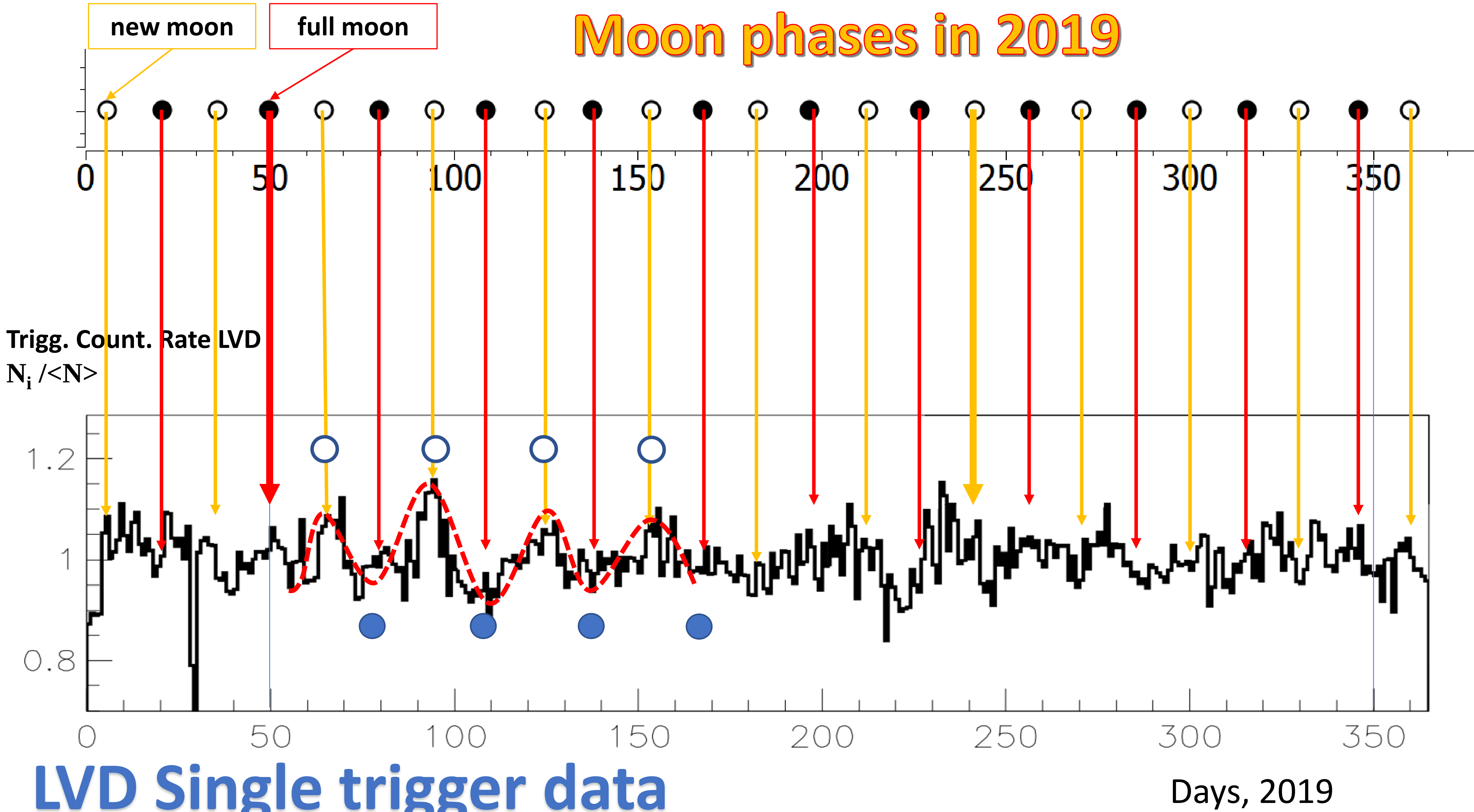

LVD Single trigger data

«Power of earthquakes»2019. Radius 250 km. Sum of events per day (magnitudes M> 2 - 7)

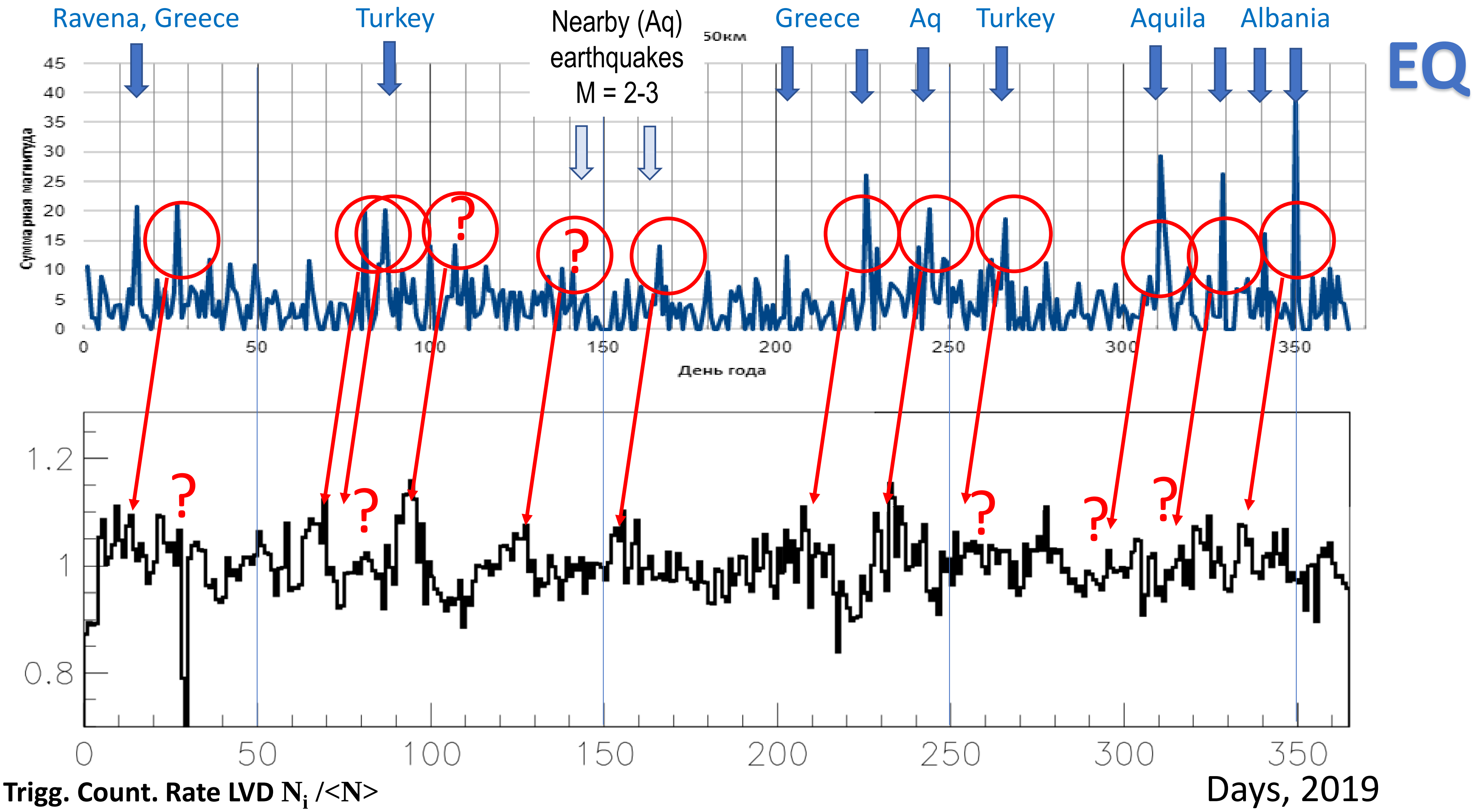

Conclusion

The change in radon concentration is influenced by geophysical, technogenic factors and seismic activity, leading to an accelerated release of Rn from the soil (especially in the condition of sedimentary rocks).

Our measurements allowed to share the total background counting rate of the LVD set-up into two components:

- variable component, associated with Radon;
- constant component, associated with the radioactivity of set-up materials and rock.

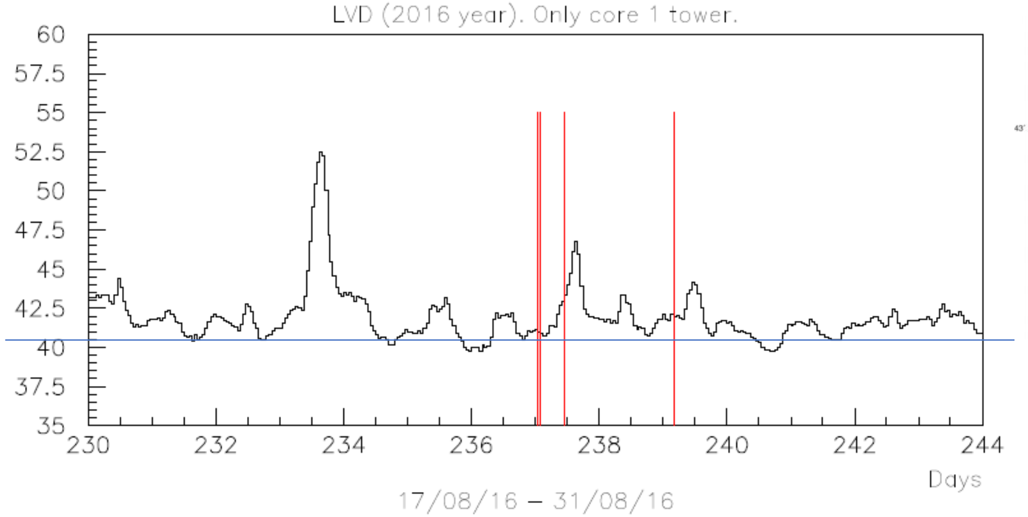

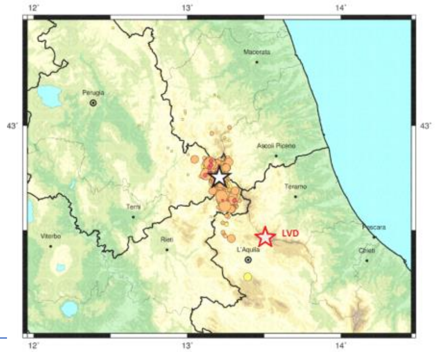

August 24, 2016

Data e Ora (UTC)	Magnitudo	Provincia/Zona
2016-08-26 04:28:25	4.8	Rieti
2016-08-24 11:50:30	4.5	Perugia
2016-08-24 02:33:28	5.4	Perugia
2016-08-24 01:37:26	4.5	Rieti
2016-08-24 01:36:32	6.0	Rieti

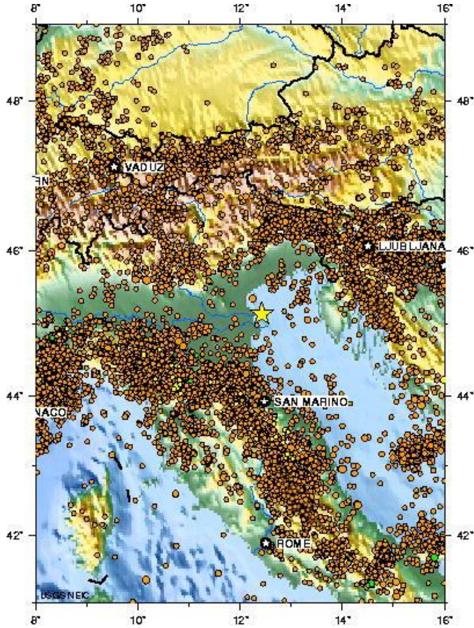

Conclusion

Factors affecting the concentration of radon in an underground laboratory.

- **Opening and closing the gates to the hall where the detector is located**: the supply ventilation creates an excess of pressure, when the gates are opened, the pressure drops and radon begins to come out of the walls intensively.
- **The passage of cars through the transport tunnel**: causes vibration of the ground, as a result of which the release of radon into the atmosphere of the hall increases.
- **Seasonal variations in radon concentration**: in summer, the water saturation of the soil is higher, which leads to an accelerated transfer of radon.
- **Seismic activity**: with deformations of the earth's crust, the number of microcracks increases, stress arises and vibration of the soil increases, which leads to a significant increase in the concentration of radon.
- **Tidal forces associated with the lunar cycle**: likely to increase the release of radon

Thank you!

«Power of earthquakes»2019. Radius 250 km. Sum of events per day (magnitudes M> 2)

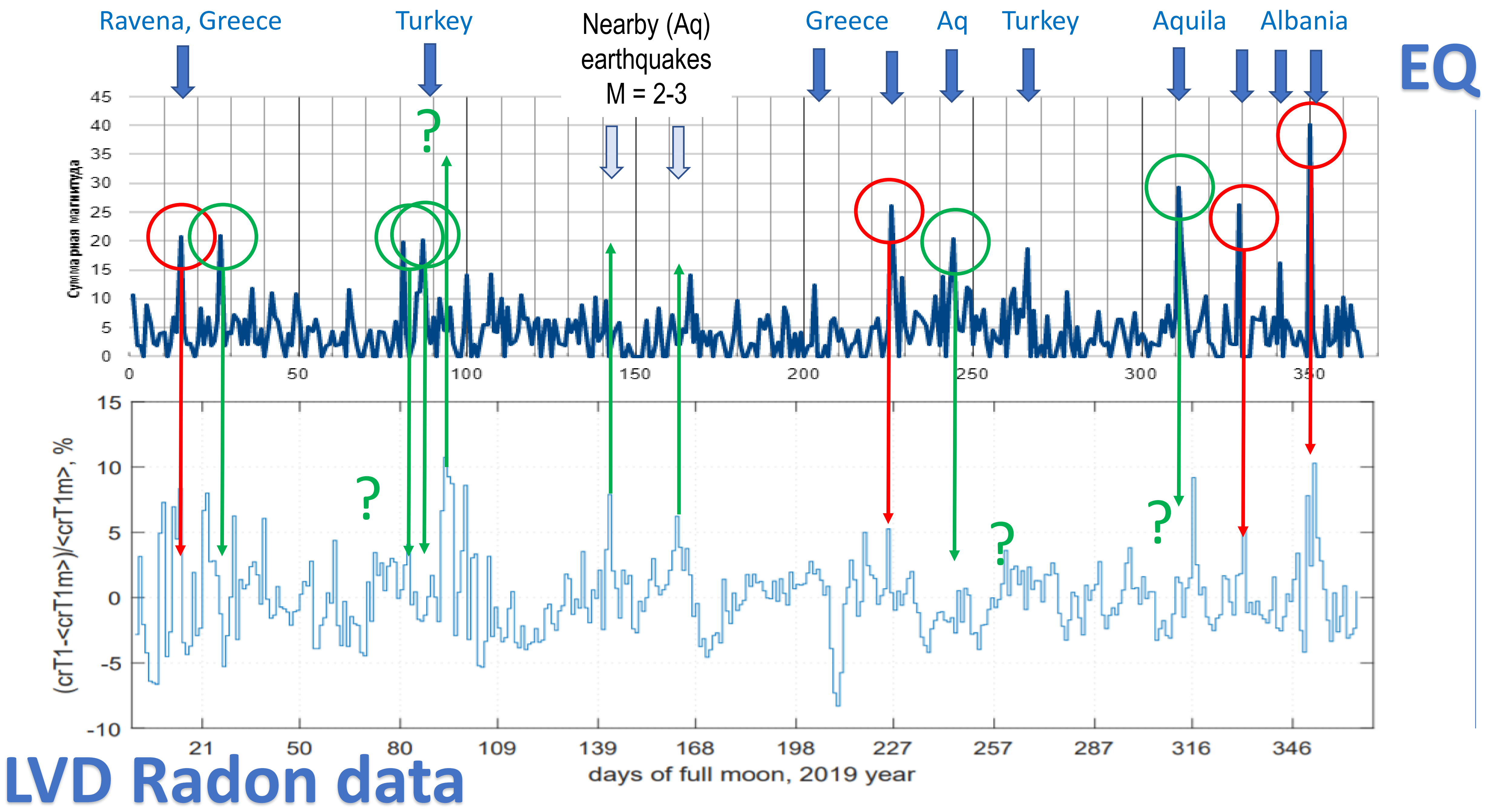

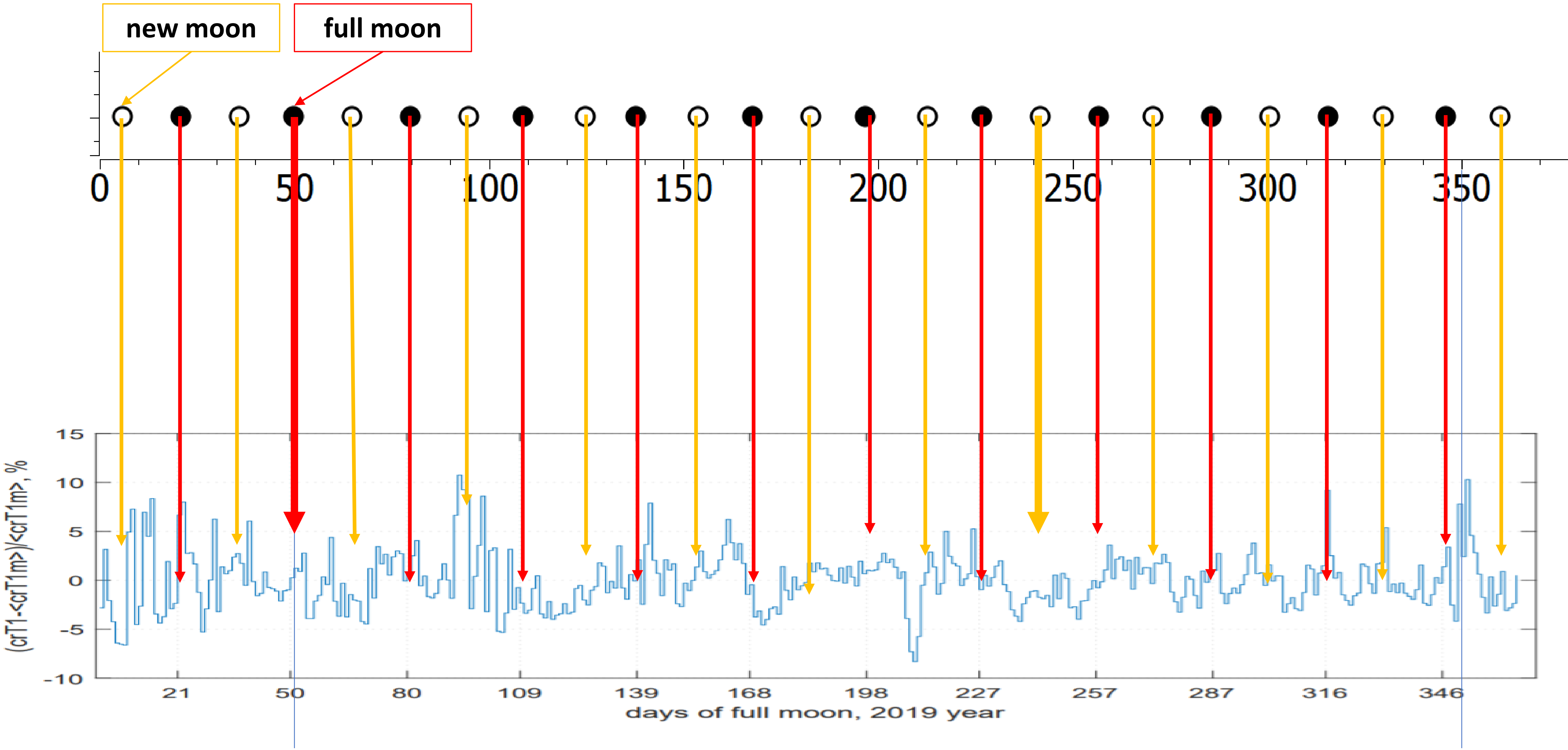
new moon
full moon
0
50
100
150
200
250
300
350
15
10
5
0
-5
-10
(crT1-<crT1m>)/<crT1m>, %
21
50
80
109
139
168
198
227
257
287
316
346
days of full moon, 2019 year

Days, 2019

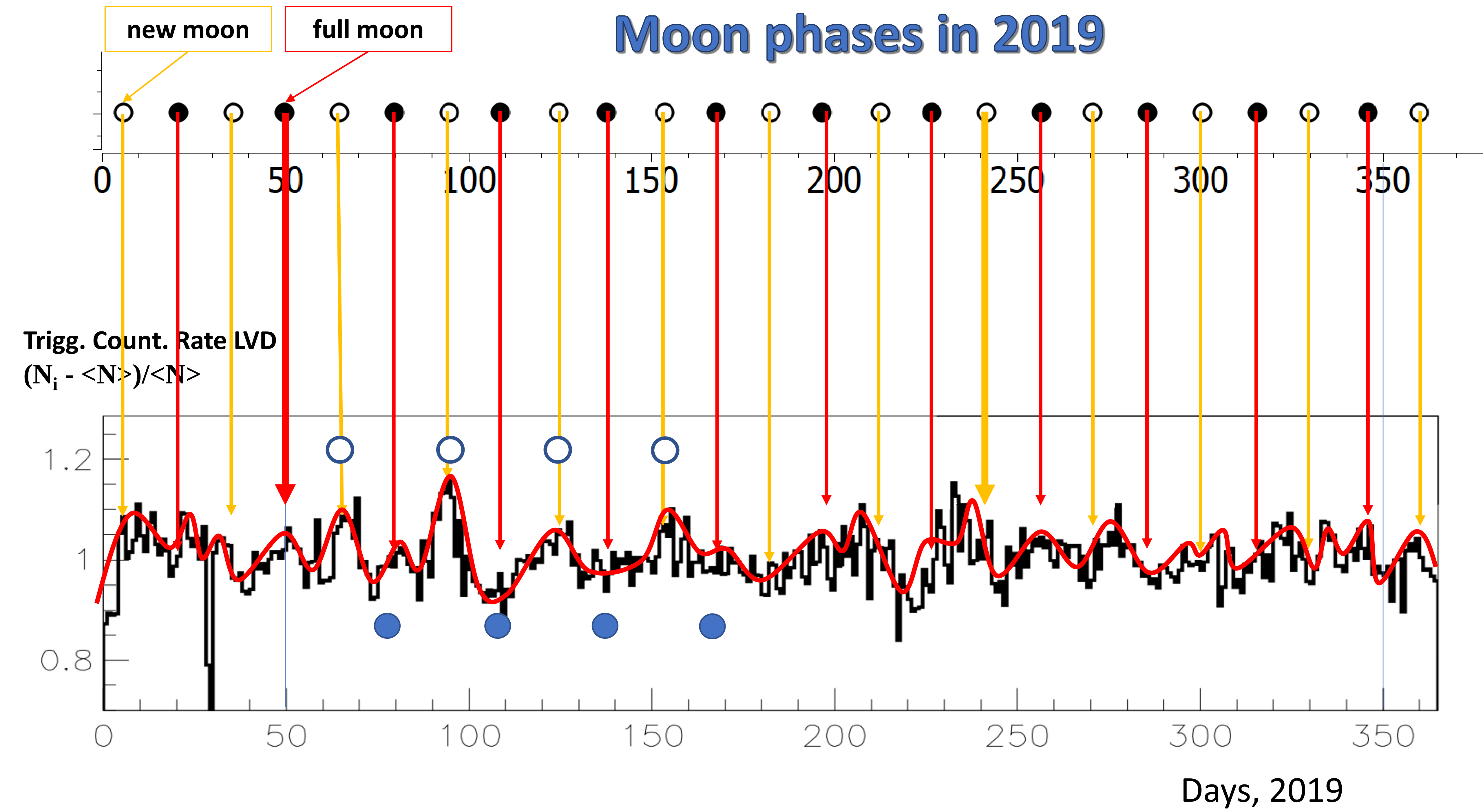

new moon
full moon
Moon phases in 2019
0
50
100
150
200
250
300
350
Trigg. Count. Rate LVD
(N_i - <N>)/<N>
1.2
1
0.8
0
50
100
150
200
250
300
350
Days, 2019